Excitation-energy dependence of the resonant Auger transitions to the $4p^4(^1D)np$ $(n=5,6)$ states across the $3d_{3/2}^{-1}5p$ and $3d_{5/2}^{-1}6p$ resonances in Kr

A. Sankari,[1,2,*] S. Alitalo,[1,†] S. Fritzsche,[1,3] J. Nikkinen,[1,‡] A. Kivimäki,[1,§] S. Aksela,[1] and H. Aksela[1]
[1]*Department of Physical Sciences, University of Oulu, P. O. Box 3000, 90014 Oulu, Finland*
[2]*Department of Physics, University of Turku, 20014 Turku, Finland*
[3]*Department of Physics, University of Kassel, Heinrich-Plett-Strasse 40, D-34132 Kassel, Germany*
(Received 20 March 2007; published 3 August 2007)

The energy dependencies of the intensities and angular distribution parameters β of the resonant Auger final states $4p^4(^1D)np$ $(n=5,6)$ of Kr were determined experimentally in the excitation-energy region of the overlapping $3d_{3/2}^{-1}5p$ and $3d_{5/2}^{-1}6p$ resonances. The experimental results were compared with the outcome of multiconfiguration Dirac-Fock calculations. Combining experimental and calculated results allowed us to study interference effects between the direct and several resonant channels that populate the $4p^4(^1D)np$ states. The inclusion of the direct channel was crucial in order to reproduce the observed energy behavior of the angular distribution parameters. It was also important to take into account experimentally observed shake transitions.

DOI: 10.1103/PhysRevA.76.022702 PACS number(s): 32.80.Hd, 32.80.Fb

I. INTRODUCTION

Resonant excitation of an inner-shell electron leads to an excited state which will mostly decay via autoionization. The process is also known as the resonant Auger effect (see the review [1]). If several resonances lie close to each other, the radiation used in excitation must have a very small bandwidth, preferably much narrower than the lifetime width of the core-excited state, so that a single resonant state can be excited selectively. Under such experimental conditions, the so-called Auger resonant Raman effect results in the line sharpening of resonant Auger transitions below the lifetime width [1]. The investigation of the resonant Auger final states using photon-induced fluorescence or electron spectroscopy then offers excellent opportunities to test our theoretical models and to understand electron correlation effects in atoms and molecules. Since the first measurement of the Auger resonant Raman effect in the vacuum ultraviolet region [2], a wealth of other studies have been performed (see, e.g., [1] and references therein).

The resonant Auger effect is especially suitable for investigating different interference mechanisms. Coherence between different resonance states, as well as the interference between resonant and direct pathways, affect the transition amplitudes describing all the processes. The way in which transition amplitudes determine angular parameters and cross sections dictates that anisotropy parameters (such as the angular distribution parameters of Auger electrons or the alignment and orientation parameters of the residual ion) are more sensitive to interference effects of different (resonant or direct) processes populating the resonant Auger final states than cross sections. This was demonstrated in a recent study by Schartner *et al.* [3], where the anisotropy and orientation parameters of three $4p^45p$ states were determined using fluorescence polarimetry with several photon energies in the region of the $3d^{-1}np$ $(n=5,6)$ resonances in Kr.

In the two-step (or stepwise) model used often in the past (see, e.g., [4]), the resonant Auger decay is described in separate steps: the first step involves resonant excitation by absorption of a photon and the following step spectator Auger decay. This model neglects the contribution of the direct channel as well as coherence effect(s) resulting from other resonances. The inadequacy of the two-step model to describe the resonant Auger decay was observed in the case of the Kr $4p^4(^1D)np$ $(n=5,6)$ states in the photon energy region of the overlapping $3d_{3/2}^{-1}5p$ and $3d_{5/2}^{-1}6p$ resonances [5], where the intensity of these groups showed traces of interference due to the lifetime broadening of the resonances. Inclusion of interference in calculations for Kr [6] showed how drastic changes anisotropy parameters (the alignment A_{20} and angular distribution parameter β) show in the region of the $3d^{-1}np$ $(n=5,6)$ excitations in Kr.

Recently, moreover, the behavior of the intensities and β parameters of the Ar $3p^4nl$ states was investigated across the $2p_{1/2}^{-1}4s$ and $2p_{3/2}^{-1}3d$ resonances in [7]. Multiconfiguration Dirac-Fock calculations including the interference due to the direct channel contribution as well as the other resonances showed that the direct channel has a negligible contribution in the energy region of these closely spaced resonances. In the case of Kr, the experimental angular distribution parameters were determined only on top of the resonances in the earlier studies [4,8], and the alignment and orientation parameters measured using photon-induced fluorescence spectroscopy (see [3] and references therein) were confined to $4p^45p$ final states. In the present study, the behavior of the β parameters is now followed across the two overlapping resonances $3d_{3/2}^{-1}5p$ and $3d_{5/2}^{-1}6p$ at photon energies 92.425 and 92.560 eV [9], respectively, for the experimentally resolvable $4p^4(^1D)np$ $(n=5,6)$ resonant Auger electron lines. The situation is illustrated in Fig. 1. The experimental results for the intensity and angular distribution parameter are com-

*anna.sankari@oulu.fi
†Present address: Oulu University of Applied Sciences, Kotkantie 1, FIN-90250 Oulu, Finland.
‡Present address: Department of Diagnostic Radiology, P. O. Box 50, 90029 Oulu University Hospital, Oulu, Finland.
§Present address: CNR-INFM, TASC Laboratory, 34012 Trieste, Italy.

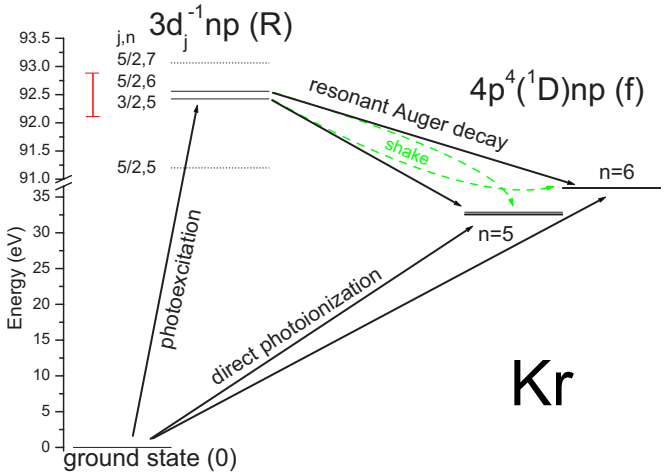

FIG. 1. (Color online) Schematic energy diagram of the different processes interfering with each other in the population of the $4p^4(^1D)np$ $(n=5,6)$ states. The investigated photon energy region is marked with the vertical (red) line in the left side of the $3d_j^{-1}np$ states. Dashed (green) arrows denote shake transitions $3d^{-1}np \rightarrow 4p^4mp$ $(n \neq m)$. Abbreviations used for atomic states are also indicated in parentheses.

pared with the multiconfiguration Dirac-Fock calculations, as well as with the β parameters published earlier [4,8].

II. EXPERIMENT

The electron spectra were measured at the gas-phase beamline I411 at the MAX-II storage ring in Lund, Sweden [10,11]. The photon bandwidth with a 10 μm monochromator exit slit was estimated to be about 10 meV, much smaller than the natural linewidths (around 80 meV [12]) of the Kr $3d^{-1}np$ resonances. Thus the Auger resonant Raman conditions were fully exploited, resulting in the line sharpening effect.

The spectra were measured with a rotatable hemispherical Scienta SES-200 electron spectrometer positioned at 0°, 54.7°, and 90° with respect to the polarization vector of incoming radiation. Using a 10 eV pass energy, the kinetic energy resolution was about 20 meV, resulting in a total experimental broadening of about 25 meV. High-resolution electron spectra were measured with photon energies from 92.12 to 92.87 eV with a 10 meV step, thus covering the overlapping $3d_{3/2}^{-1}5p$ and $3d_{5/2}^{-1}6p$ resonances, as shown by the vertical line in Fig. 1. The spectra were corrected for the variations in pressure and incoming photon flux.

The emission of Auger electrons is nonisotropic in cases where the initial vacancy is in a subshell with angular momentum $j>1/2$. This anisotropy results from the excitation or ionization leaving the atom or ion aligned with respect to the exciting beam. The angular distribution parameter β describing the anisotropy of an Auger electron depends on the alignment of the atom (or ion) and on the matrix elements of Auger decay together with the angular moments of the initial and final states. [13]

The intensity I_θ of emitted Auger electrons at an angle θ with respect to the polarization vector of incoming radiation

TABLE I. Assignment and binding energies (in eV) of the $4p^4(^1D)np$ $(n=5,6)$ lines. The labels are used in the text and figures.

	LS term	Label	Binding energy
$4p^4(^1D)5p$	$^2D_{3/2}$, $^2P_{1/2}$, $^2D_{5/2}$ [a]	1	32.874[a]
	$^2P_{3/2}$ [a]	2	32.623[a]
	$^2F_{7/2}$ [a]	3	32.561[a]
	$^2F_{5/2}$ [a]	4	32.496[a]
$4p^4(^1D)6p$	$^2D_{3/2}$, $^2D_{5/2}$ [b]	5	36.335
	$^2P_{1/2}$ [b]	6	36.276
	$^2P_{3/2}$, $^2F_{7/2}$	7	36.237
	$^2F_{5/2}$ [b]	8	36.209

[a]From Ref. [16].
[b]Identical with the assignment given in [8].

is related to the total intensity I_{tot} of the emitted electrons as (see, e.g., [8,13])

$$I_\theta = \frac{I_{\mathrm{tot}}}{4\pi}[1+\beta P_2(\cos\theta)], \tag{1}$$

where $P_2(x)$ is the second-order Legendre polynomial, and β is the angular distribution parameter. According to this relation, the Auger electron intensity measured at two angles would be sufficient for the determination of β parameters. Spectra from three angles enabled us to determine more reliably the angular distribution parameters, which are given as averages of the three possible determinations, and also provided us with error bars, which are given as a maximum deviation from the mean value. In the normalization of the spectra measured at different angles, the previously measured β parameters for $4p^4(^1D)5p$ lines [4] were used.

From the experimental spectra, the binding energies of the $4p^4(^1D)6p$ states were also determined with an accuracy of ±2 meV. The energies of the $4p^4(^1D)5p$ lines are well known from optical data [14] as well as from the $4s$ photoelectron satellite spectrum [15,16]. The binding energies in Table I were determined with respect to the $4s$ photoelectron line at 27.512 eV. As in [15], we used the experimental angular distribution parameters to identify the $4p^4(^1D)6p$ lines by comparing them and their energy behavior with our calculations. The obtained assignment together with the corresponding labels and binding energies is given in Table I. The assignments of the $4p^4(^1D)6p$ states given in Table I are identical with those of Ref. [8], except for line 7, which differs partly from the earlier assignments [8,15]. The binding energies for lines 6 and 7 coincide with the previously given values [16] within 1 meV.

III. THEORY

The theoretical method exploited in this work was the same as in [7]. The relativistic wave functions for ground, intermediate, and final states were calculated in the multiconfiguration Dirac-Fock approximation by means of the

GRASP92 program [17], where atomic state functions (ASFs) are estimated as linear combinations of jj-coupled configuration state functions (CSFs). By converting these rather heavily mixed ASFs from the jj-coupled basis into the LSJ basis [18], we obtained fairly pure (>85.%) LS terms for the $4p^4(^1D)np$ states given in Table I.

In the intermediate state (R), only six $3d^{-1}np$, $n=5,6$ ($J=1$), states were included. The $3d_{3/2}^{-1}np$ resonances are composed of two very mixed states of $3d_{3/2}^{-1}np_{1/2}$ and $3d_{3/2}^{-1}np_{3/2}$ composition in the jj-coupled basis. The occupation probability of one of them is often very small compared to the other one, which explains why only one of the resonances is seen in the experiments. In our calculations, the second $3d_{3/2}^{-1}5p$ resonance obtained only 7% of the transition probability of the other. Nonetheless, it was included in the calculations of the transition amplitudes. In the final state (f), the configurations $4p^45p$ and $4p^46p$ were included in the calculation, resulting in a total of 42 final states. Calculating both $5p$ and $6p$ states together allowed the mixing of these states, but the effects of this configuration interaction (i.e., the mixing of the states) remained small.

The total transition amplitude $D(h\nu,f)$ from the ground state (0) to a given resonant Auger final state (f) as a function of the exciting photon energy ($h\nu$) can be obtained from the equation (see, e.g., [3,5,7])

$$D(h\nu,f) = \langle f|\mathbf{D}|0\rangle + \sum_R \frac{\langle f|\mathbf{V}|R\rangle\langle R|\mathbf{D}|0\rangle}{h\nu - E_R + \imath\Gamma_R/2}, \tag{2}$$

where the latter part of the sum describes the resonant pathway and contains also the dependence of the energy (E_R) and inherent lifetime width (Γ_R) of a resonance R. The first term of the sum is the direct photoionization from the ground state, which was calculated (as in [7]) using the nonorthogonality of separately optimized orbitals in the ground and final states. This was done with the recently implemented PHOTO component [19] of the RATIP program using the orbitals given by GRASP92. The RATIP program [20] offered us tools to calculate also the other amplitudes required in Eq. (2).

The REOS99 component [21] was used to evaluate the photoexcitation probabilities from the ground state to the intermediate (or resonance) states R, i.e., the transition probabilities $\langle R|\mathbf{D}|0\rangle$ mediated by the dipole operator $\mathbf{D}$. To facilitate comparison with the experimental results, however, the energies [9] and line broadenings [12] were used from previous measurements. For the same reason, the intensities of the $3d_{3/2}^{-1}5p$ and $3d_{5/2}^{-1}6p$ resonances were scaled in order to correspond to the experimentally observed intensity ratios [9].

The resonant Auger transitions $\langle f|\mathbf{V}|R\rangle$, where $\mathbf{V}=\mathbf{V}_{\text{Coulomb}}$ is the Coulomb operator, were calculated by using the AUGER component [22] of the RATIP package. Unfortunately, this program calculates transition probabilities only for two-electron processes. However, the shake transitions $3d^{-1}np \rightarrow 4p^4mp$, $n \neq m$, have been shown to have remarkable probabilities in Kr [23], and even though some intensity was obtained also for $3d^{-1}np \rightarrow 4p^4mp$ ($n \neq m$) transitions through the mixing of the states, they had only a minor contribution in comparison with the dominating spectator transitions ($n=m$). These shake transitions occur due to the relaxation of the one-electron orbitals in the course of the Auger decay and their transition probabilities can be approximated as (see, e.g., [1,24])

$$\langle 4p^4mp\epsilon l|\mathbf{V}|3d^{-1}n'p'\rangle \approx \langle mp|n'p'\rangle\langle 4p^4np\epsilon l|\mathbf{V}|3d^{-1}n'p'\rangle, \tag{3}$$

where the notation $|n'p'\rangle$ is used to emphasize the nonorthogonality between the orbital sets of the resonance and final states.

TABLE II. Overlaps $\langle nl|m'l'\rangle$ used in the calculation of relaxation effects. Notation $np-$ stands for $np_{l/2}$ orbital and np for $np_{3/2}$.

	$m'l'$			
nl	$5p-$	$5p$	$6p-$	$6p$
$5p-$	0.999		0.032	
$5p$		0.946		0.324
$6p-$	−0.032		0.999	
$6p$		−0.324		0.946

To study the effect of relaxation in our results, we performed two kinds of calculations. Calculation A, which includes the effects of the configuration interactions, was performed without any relaxation, whereas calculation B takes into account the relaxation by utilizing the so-called relaxed Auger amplitudes

$$\langle f_n|\mathbf{V}|R\rangle_B = \langle np|n'p'\rangle\langle f_n|\mathbf{V}|R\rangle_A + \langle np|m'p'\rangle\langle f_m|\mathbf{V}|R\rangle_A, \tag{4}$$

as obtained from the amplitudes of calculation A, where the subscript n (or m) refers to the np (or mp) orbital of the excited electron in the final state. The overlaps $\langle nl|m'l'\rangle$ used are given in Table II.

To investigate the contribution of the direct channel, the calculation of the transition amplitudes [cf. Eq. (2)] was carried out with and without the first term of the sum for both calculations A and B. Below, we shall use the subscript d to denote the calculations in which the direct channel is included (calculations A_d and B_d), while A and B are used to refer to those calculations without the direct contribution. Therefore, calculations A and B show the effect of the interference between different resonance channels, whereas the difference between the calculations with or without direct channel manifests the importance of taking the direct contribution into account.

In the present computations, however, the direct amplitudes could be included only for the states with $J=1/2$ or $3/2$, although states with $J>3/2$ have also been observed in the Kr $4s$ photoelectron satellite spectrum [15,16]. This restriction arises from the fact that, for states with $J>3/2$, the computation of the direct photoionization amplitudes requires a full treatment of the relaxation.

The direct amplitudes (as well as the photoexcitation probabilities) were calculated in the dipole approximation using both velocity (Coulomb) and length (Babushkin) gauges. Usually, the direct amplitudes obtained in the veloc-

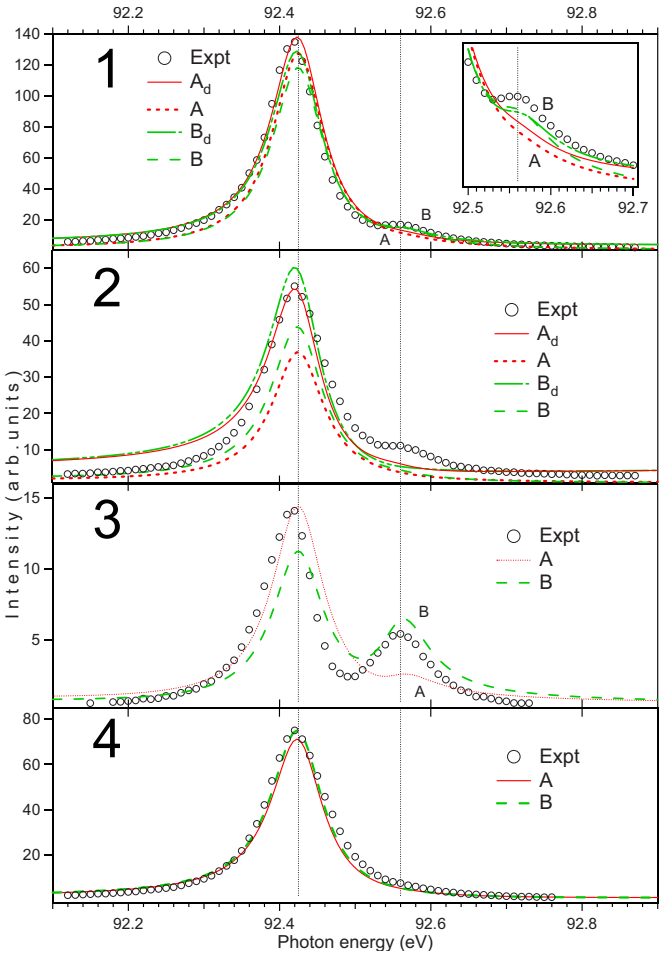

FIG. 2. (Color online) Experimental (dots) and theoretical intensities of the $4p^4(^1D)5p$ lines as a function of exciting photon energy. The experimental curves are from the measurements at 54.7°. The inset in the upper corner shows the magnification of the line 1 near the $3d_{5/2}^{-1}6p$ resonance. The positions of the $3d_{3/2}^{-1}5p$ and $3d_{5/2}^{-1}6p$ resonances at 92.425 and 92.560 eV, respectively, are marked by vertical lines. See Table I for the assignment of the lines.

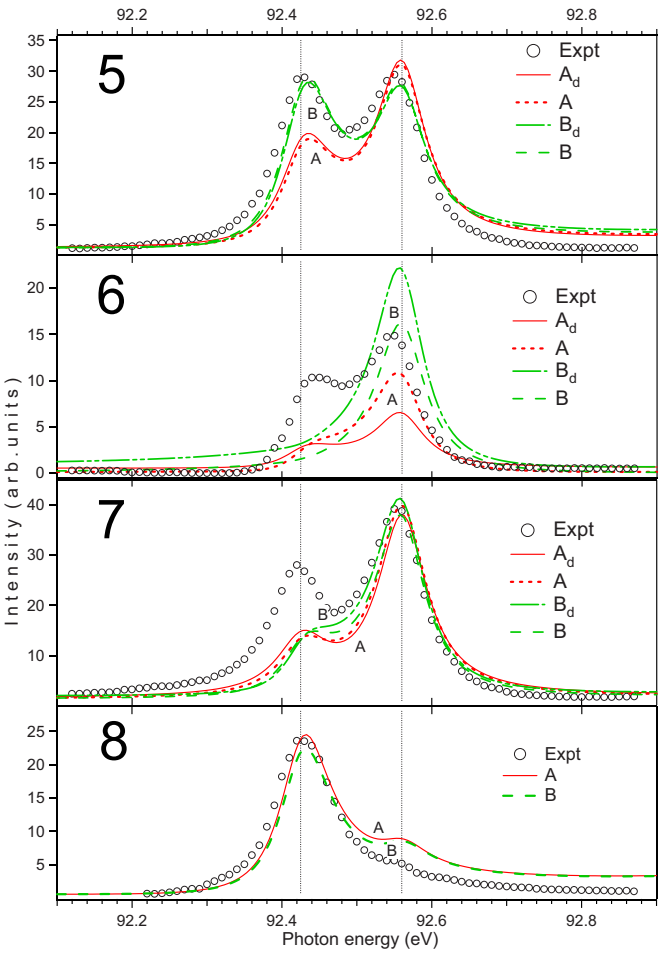

FIG. 3. (Color online) Experimental (dots) and theoretical intensities of the $4p^4(^1D)6p$ lines as a function of exciting photon energy. As in Fig. 2, the experimental results are from measurements at 54.7°, and the positions of the $3d_{3/2}^{-1}5p$ and $3d_{5/2}^{-1}6p$ resonances are marked by vertical lines. See Table I for the assignment of the lines.

ity gauge are slightly larger than the ones obtained in the length gauge. The results in this work containing the direct contribution were calculated in the velocity gauge, which gave the larger contribution. For one state, namely, $4p^4(^1D)5p\ ^2P_{3/2}$ (line 2), the gauge difference was more pronounced than for the others, and the results of the angular distribution parameter are given in both velocity and length gauges for this state.

In the case of overlapping final states, which we could not resolve experimentally (lines 1, 5, and 7), we calculated the corresponding theoretical intensity as the sum of the intensities of these states and the angular anisotropy parameter as an intensity-weighted average from the individual angular distribution parameters of the states involved.

IV. RESULTS AND DISCUSSION

The experimental and calculated intensities of the $4p^4(^1D)5p$ and $6p$ lines are shown in Figs. 2 and 3, respectively. These measurements were carried out at 54.7°. Results for angular distribution parameters, as well as the previously published values [4,8], are shown in Figs. 4 and 5 and the experimental results seem to be in good agreement. Note that the intensities far from the resonances are rather low, and that the errors in the region below and above these two resonances $3d_{3/2}^{-1}5p$ and $3d_{5/2}^{-1}6p$ are larger than on top or in between the resonances. In addition, the weakest line of all, namely, line 6 $[4p^4(^1D)6p\ ^2P_{1/2}]$, gave rise to such large error bars in the angular distribution parameter that it is pointless to show the results. Without doubt, however, the β values were clearly positive (in accordance with the value 1.2 in [8] at the latter resonance) which enabled us to identify and confirm the assignment given for this line. Instead of β for line 6, the experimental intensity-weighted average of the angular distribution parameters of the $4p^4(^1D)6p$ states is shown in Fig. 5, which shows much less pronounced interference effects than are obtained for the individual lines. This demonstrates again the importance of high resolution in these kinds of studies, i.e., for analyzing the interplay between various channels populating the same final state.

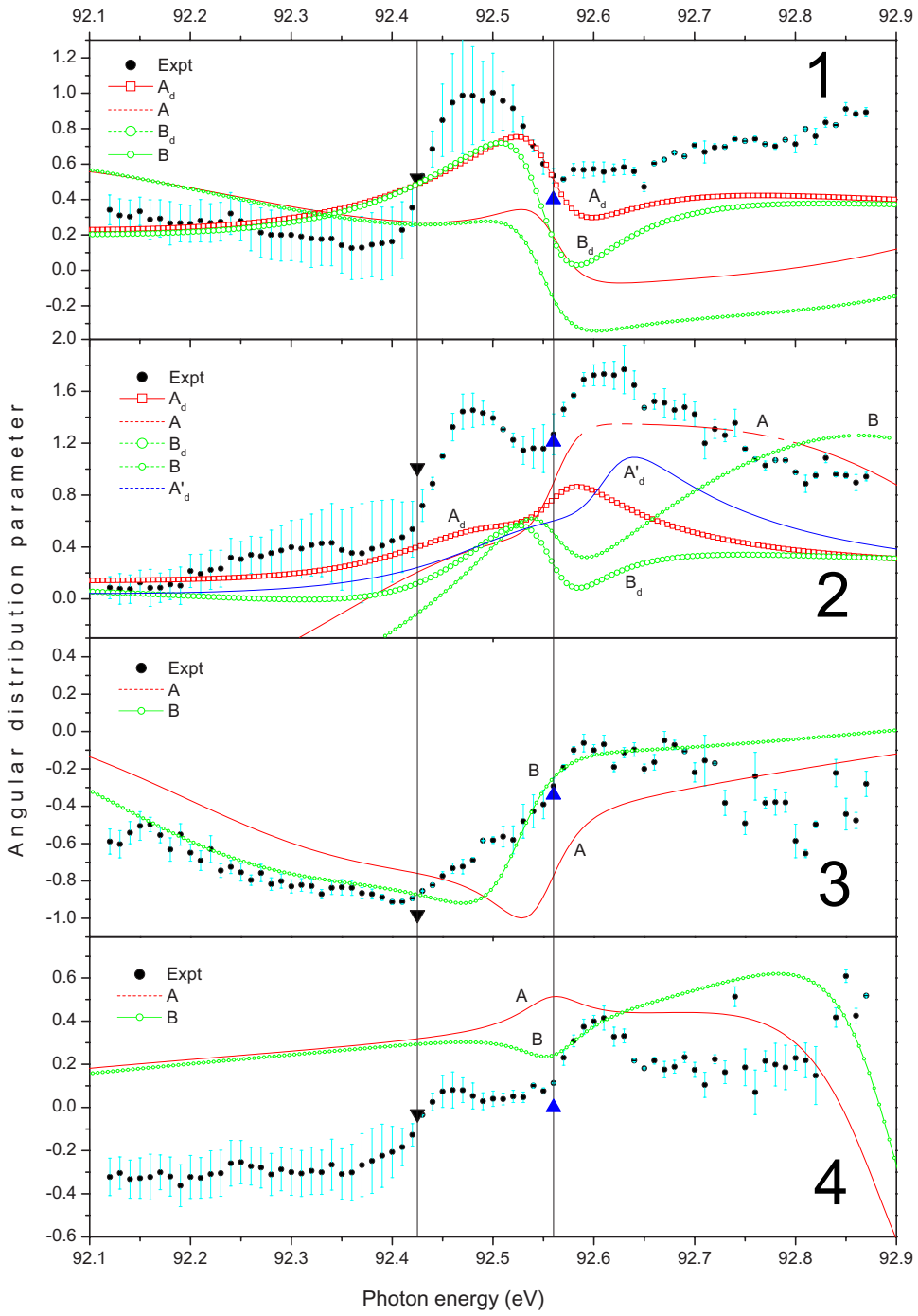

FIG. 4. (Color online) Experimental (dots) and theoretical angular distribution parameters β of the $4p^4(^1D)5p$ lines as a function of exciting photon energy. The previously published values are from Refs. [4] (downward triangles) and [8] (upward triangles). For line 2 also the direct channel calculation in the length gauge (A'_d) is shown. See Table I for the assignment of the lines.

The experimental intensities of the $4p^4(^1D)5p$ lines in Fig. 2 show clearly the dominance of the spectator Auger transitions at the $3d_{3/2}^{-1}5p$ resonance. Thus, the expected effects of relaxation are small, especially for lines 1 and 4.

For line 3 [$4p^4(^1D)5p\ ^2F_{7/2}$], the inclusion of relaxation improves both the intensity and the angular distribution parameter shown in Fig. 4. In contrast, for line 4, the final state $4p^4(^1D)5p\ ^2F_{5/2}$, it is hard to say which calculation is better: Differences between the approximations occur above the $3d_{5/2}^{-1}6p$ resonance, where, unfortunately, the experimental angular distribution parameters show some deviations. This is quite a general trend for all the states involved: the largest deviations between different approximations occur usually far from the resonances, where none of the resonant pathways dominates over the others. Outside the resonances, of course, these lines have only small cross sections, and other $4s$ photoelectron satellite lines complicate the detection of the lines.

The deviation between the calculated and observed β parameters of line 4 below the $3d_{5/2}^{-1}6p$ resonance manifests the absence of the direct contribution in our calculations. Both lines 3 and 4 [$4p^4(^1D)5p\ ^2F_{7/2}$ and $^2F_{5/2}$, respectively] are observed in the $4s$ photoelectron satellite spectrum [16], and our calculation fails to predict any direct contribution for these lines. For line 3, the interference between the resonances has the dominant role in the investigated energy re-

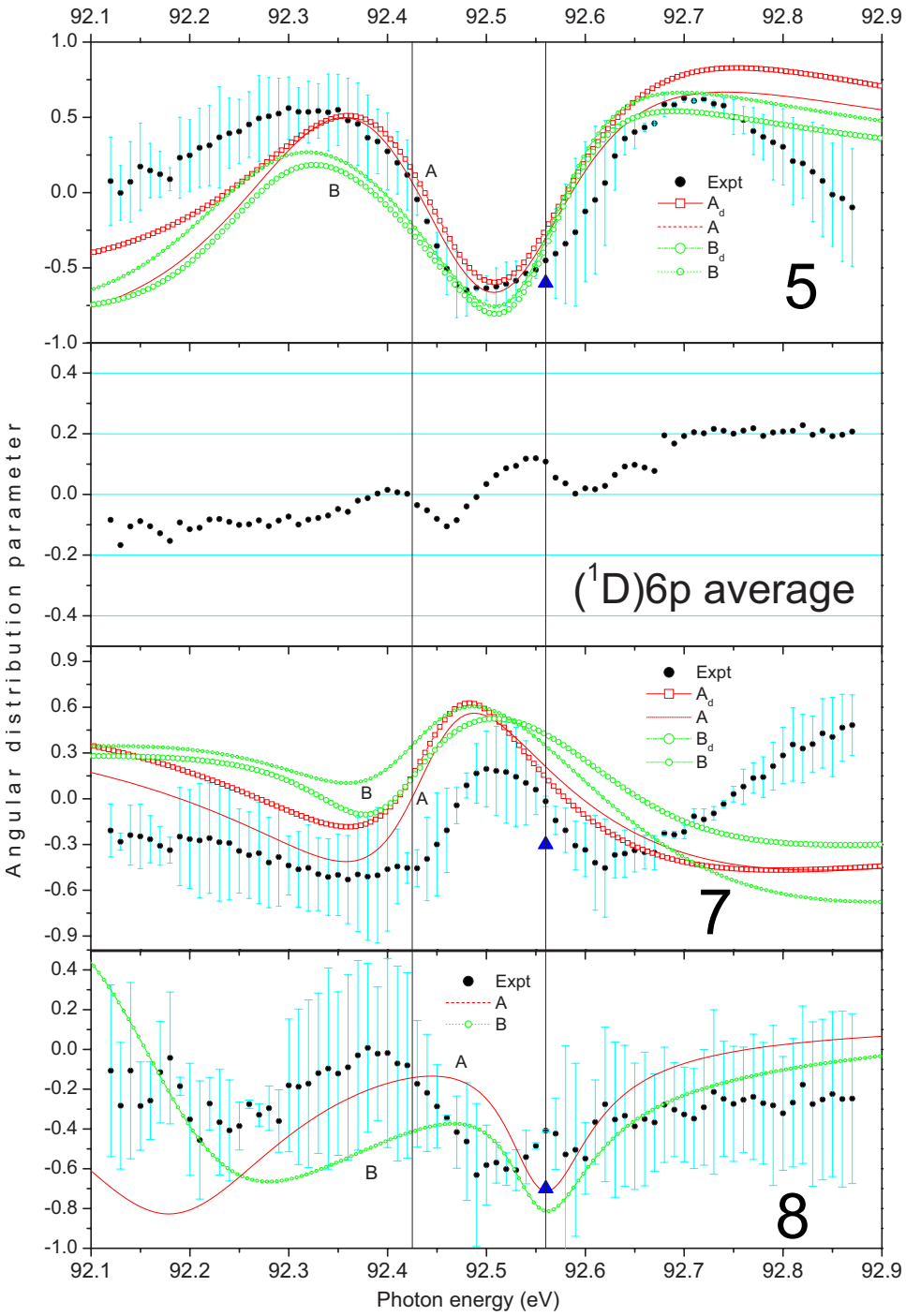

FIG. 5. (Color online) Experimental (dots) and theoretical angular distribution parameters β of the $4p^4(^1D)6p$ lines as in Fig. 4. The previously published values are from Ref. [8] (upward triangles). Instead of results for β parameter of line 6, the intensity-weighted average for all $4p^4(^1D)6p$ lines is shown. See Table I for the assignment of the lines.

gion, whereas, for line 4, for which the $3d_{3/2}^{-1}5p$ resonance clearly dominates over the $3d_{5/2}^{-1}6p$ resonance, the neglect of the direct channel is more pronounced in the absence of other interfering channels.

Line 1 is, in fact, a superposition of three $4p^4(^1D)5p$ final states, $^2D_{3/2}$, $^2P_{1/2}$, and $^2D_{5/2}$. For this line, the asymmetry of the intensity behavior is nicely reproduced by including the direct channel into the calculations, and the incorporation of relaxation effects improves even further the agreement between experiment and theory at the $3d_{5/2}^{-1}6p$ resonance, as shown by the inset in Fig. 2. Some discrepancies still remain in the angular distribution parameter above the resonances. This discrepancy is most likely due to the fact that our calculations did not include the $3d^{-1}7p$ resonances in the intermediate state, from which the first one, $3d_{5/2}^{-1}7p$ at 93.063 eV [9], is only 0.503 eV above the $3d_{5/2}^{-1}6p$ resonance as seen from Fig. 1. A similar discrepancy is clearly visible also for line 7 [states $4p^4(^1D)6p\ ^2F_{7/2}$ and $^2P_{3/2}$] in Fig. 5.

In the case of line 2 [$4p^4(^1D)5p\ ^2P_{3/2}$], our calculations fail in including both the direct channel and relaxation. The Fano profile produced by these calculations, which include the direct channel, is more asymmetric than the experimental intensity profile, and the shoulder at the $3d_{5/2}^{-1}6p$ resonance is not well reproduced by either calculation A or B. By studying the more sensitive β parameter and the theoretical results with direct amplitudes from the velocity and length gauges

(calculations A_d and A'_d, respectively) we find that the smaller direct amplitude (from length gauge) gives a closer resemblance with the experimental values. Some discrepancies still remain above the resonances, because the relaxation effects predicted by calculation B are too low, and deviations possibly occur also due to the $3d_{5/2}^{-1}7p$ resonance neglected in the calculations.

The behavior of the $4p^4(^1D)6p$ lines is more interesting, being much more pronounced and complicated than the behavior of the corresponding $5p$ lines. Whereas the intensity-weighted average of the angular distribution parameters of the $4p^4(^1D)5p$ states is similar to the angular distribution parameter of the (most intense) line 1, that of the $4p^4(^1D)6p$ states in Fig. 5 loses most of the anisotropy, not to mention the interference effects, which change from line to line.

The study of the $4p^4(^1D)6p$ lines is by no means a trivial task experimentally, since 47.7% of the intensity from the $3d_{5/2}^{-1}6p$ intermediate state goes to $4p^47p$ states through a shakeup process, and only a quarter is left for the $4p^46p$ states after other shake processes [23]. In the resonant Auger electron spectrum, some $4p^45d$, $6d$, $7s$, and $7p$ photoelectron satellites have nearly the same binding energy as the $4p^4(^1D)6p$ lines, complicating the study even further. Due to this overlap of several final states, the $4p^4(^1D)6p$ lines have not been identified from the $4s^{-1}$ satellite spectrum with certainty. Near the resonances, as in the energy region studied in this work, these difficulties are possible to overcome even though not without a trace: Due to the smaller intensities and background of other satellite lines, the error bars of the angular distribution parameters are larger for the $4p^4(^1D)6p$ lines than for the $4p^4(^1D)5p$ lines.

Large error bars make it difficult to compare the details of our calculations with the experimental values, especially when the differences of the calculations near the resonances are small. For line 5 $[4p^4(^1D)6p\ ^2D_{3/2}+^2D_{5/2}]$ the intensity behavior implies that the relaxation improves our theoretical prediction, but the asymmetry is overestimated. This applies to calculations both with and without the direct channel, suggesting that there is another resonance channel, i.e., a shake-down process from the close-lying $3d_{5/2}^{-1}7p$ resonance. The more sensitive angular distribution parameter has some deviations only outside the resonances, where below the resonances calculation A_d has the closest values to those of the experiment. This applies also to the line 7 $[4p^4(^1D)6p\ ^2F_{7/2}+^2P_{3/2}]$, for which the relaxation even degrades the intensity ratios at the resonances. The latter can be traced back to the relaxation failure of line 2 $[4p^4(^1D)5p\ ^2P_{3/2}]$, since these states share the intensity due to the relaxation of the (one-electron) orbitals. This can only be due to certain difficulties either in the simplified evaluation of the transition amplitudes [cf. Eq. (3)], or in the representation of the orbitals that were used for calculating the overlaps. The orbitals were optimized together, but the absence of higher orbitals affects their quality.

Also, the relaxation of line 6 $[4p^4(^1D)6p^2P_{1/2}]$ worsens the intensity behavior well predicted by calculation A_d. However, the corresponding $5p$ state overlaps with the $^2D_{3/2}$ and $^2D_{5/2}$ states (line 1), and therefore it is impossible to compare the experimental data and to say whether the relaxation prediction fails also for the $4p^4(^1D)5p\ ^2P_{1/2}$ state. In the absence of reliable results for the angular distribution parameter, no conclusions can be drawn for line 6. For the final state $4p^4(^1D)6p\ ^2F_{5/2}$ (line 8), the theoretically predicted direct channel is negligible, and both the calculations A and B overestimate its intensity at the $3d_{5/2}^{-1}6p$ resonance. Nonetheless, both the calculations seem to follow the behavior of the angular distribution parameter within the (rather large) error bars.

According to these results, we find that the inclusion of the direct channel in the calculation is important, even though our calculation overestimated its contribution for the $4p^4(^1D)6p\ ^2P_{3/2}$ state and could not predict any contribution for the states with $J>3/2$. When taking into account other resonance pathways also, relaxation processes (shake-transitions) should be incorporated in the theoretical treatment.

V. CONCLUSIONS

The intensity and angular distribution parameter β of the $4p^4(^1D)np$ $(n=5,6)$ lines of Kr were determined from high-resolution resonant Auger electron spectra as a function of the exciting photon energies in the region of the overlapping $3d_{3/2}^{-1}5p$ and $3d_{5/2}^{-1}6p$ resonances, and compared with results of multiconfiguration Dirac-Fock calculations. These computations include interference effects originating from the contribution of the direct channel and other resonance channels. The assignments for the $4p^4(^1D)6p$ lines were confirmed, and the binding energies for all these lines were given. Energy-dependent results for the β parameters illustrated the importance of accounting for interference effects between the direct and resonance pathways. The remaining discrepancies between the calculations and experimental values suggest that further improvements still remain to be made in the theoretical description of the (continuum-embedded) resonances as well as the final scattering states, in order to predict different interference mechanisms properly.

ACKNOWLEDGMENTS

The assistance of the MAX-lab staff is greatfully acknowledged. This work has been supported by the Finnish Academy for Natural Sciences, National Graduate School in Materials Physics (NGSMP), and by the European Community Access to Research Infrastructure action of the Improving Human Potential Program. S.F. acknowledges support by the DFG under Project No. FR 1251/13.

[1] B. G. Armen, H. Aksela, T. Åberg, and S. Aksela, J. Phys. B **33**, R49 (2000).
[2] A. Kivimäki, A. Naves de Brito, S. Aksela, H. Aksela, O.-P. Sairanen, A. Ausmees, S. J. Osborne, L. B. Dantas, and S. Svensson, Phys. Rev. Lett. **71**, 4307 (1993).
[3] K.-H. Schartner, R. H. Schill, D. Hasselkamp, S. Mickat, S. Kammer, L. Werner, S. Klumpp, A. Ehresmann, H. Schmoranzer, B. M. Lagutin, and V. L. Sukhorukov, J. Phys. B **38**, 4155 (2005).
[4] H. Aksela, J. Jauhiainen, E. Nõmmiste, S. Aksela, S. Sundin, A. Ausmees, and S. Svensson, Phys. Rev. A **54**, 605 (1996).
[5] E. Kukk, H. Aksela, A. Kivimäki, J. Jauhiainen, E. Nõmmiste, and S. Aksela, Phys. Rev. A **56**, 1481 (1997).
[6] B. M. Lagutin, I. D. Petrov, V. L. Sukhorukov, S. Kammer, S. Mickat, R. Schill, K.-H. Schartner, A. Ehresmann, Yu. A. Shutov, and H. Schmoranzer, Phys. Rev. Lett. **90**, 073001 (2003).
[7] S. Fritzsche, J. Nikkinen, S.-M. Huttula, H. Aksela, M. Huttula, and S. Aksela, Phys. Rev. A **75**, 012501 (2007).
[8] S.-M. Huttula, S. Alitalo, H. Aksela, S. Heinäsmäki, A. Kivimäki, J. Tulkki, M. Jurvansuu, E. Nõmmiste, and S. Aksela, Chem. Phys. **289**, 81 (2003).
[9] G. C. King, M. Tronc, F. H. Read, and R. C. Bradford, J. Phys. B **10**, 2479 (1977).
[10] M. Bässler, J.-O. Forsell, O. Björneholm, R. Feifel, M. Jurvansuu, S. Aksela, S. Sundin, S. L. Sorensen, R. Nyholm, A. Ausmees, and S. Svensson, J. Electron Spectrosc. Relat. Phenom. **101-103**, 953 (1999).
[11] M. Bässler, A. Ausmees, M. Jurvansuu, R. Feifel, J.-O. Forsell, P. de Tarso Fonseca, A. Kivimäki, S. Sundin, S. L. Sorensen, R. Nyholm, O. Björneholm, S. Aksela, and S. Svensson, Nucl. Instrum. Methods Phys. Res. A **469**, 382 (2001).
[12] O.-P. Sairanen, A. Kivimäki, E. Nõmmiste, H. Aksela, and S. Aksela, Phys. Rev. A **54**, 2834 (1996).
[13] N. M. Kabachnik and I. P. Sazhina, J. Phys. B **17**, 1335 (1984).
[14] C. E. Moore, *Atomic Energy Levels* (U.S. GPO, Washington, D. C., 1971), Vol. II.
[15] A. Caló, S. Atanassova, R. Sankari, A. Kivimäki, H. Aksela, and S. Aksela, J. Phys. B **39**, 4169 (2006).
[16] S. Alitalo, A. Kivimäki, T. Matila, K. Vaarala, H. Aksela, and S. Aksela, J. Electron Spectrosc. Relat. Phenom. **114-116**, 141 (2001).
[17] F. A. Parpia, C. Froese Fischer, and I. P. Grant, Comput. Phys. Commun. **94**, 249 (1996).
[18] G. Gaigalas, T. Zalandaukas, and S. Fritzsche, Comput. Phys. Commun. **157**, 239 (2004).
[19] S. Fritzsche, A. Surzhykov, and T. Stöhlker, Phys. Rev. A **72**, 012704 (2005).
[20] S. Fritzsche, J. Electron Spectrosc. Relat. Phenom. **114-116**, 1155 (2001); S. Fritzsche, Phys. Scr., T **100**, 37 (2002).
[21] S. Fritzsche, C. Froese Fischer, and C. Z. Dong, Comput. Phys. Commun. **124**, 340 (2000).
[22] S. Fritzsche, B. Fricke, and W.-D. Sepp, Phys. Rev. A **45**, 1465 (1992).
[23] J. Jauhiainen, H. Aksela, O.-P. Sairanen, E. Nõmmiste, and S. Aksela, J. Phys. B **29**, 3385 (1996).
[24] S. B. Whitfield, J. Tulkki, and T. Åberg, Phys. Rev. A **44**, R6983 (1991).